Observer Design for a Nonlinear Neuromuscular System with Multi-rate Sampled and Delayed Output Measurements

Qiang Zhang, Zhiyu Sheng, Kang Kim, Nitin Sharma

***Abstract*—Robotic devices and functional electrical stimulation (FES) are utilized to provide rehabilitation therapy to persons with incomplete spinal cord injury. The goal of the therapy is to improve their weakened voluntary muscle strength. A variety of control strategies used in these therapies need a measure of participant's volitional strength. This informs the robotic or an FES device to modulate assistance proportional to the user's weakness. In this paper we propose an observer design to estimate ankle kinematics that are elicited volitionally. The observer uses a nonlinear continuous-time neuromuscular system, which has multi-rate sampled output measurements with non-uniform and unknown delays from various sensing modalities including electromyography, ultrasound imaging, and an inertial measurement unit. We assume an allowable maximum value of unsynchronized sampling intervals and non-uniform delays. By constructing a Lyapunov-Krasovskii function, sufficient conditions are derived to prove the exponential stability of the estimation error. Numerical simulations are provided to verify the effectiveness of the designed observer.**

I. Introduction

Each year in the United States 17,000 people experience a spinal cord injury (SCI) [1], and the majority of the cases are incomplete spinal cord injury (iSCI). Unlike persons with complete SCI, persons with iSCI may have voluntary control of limbs but the strength is weakened compared to able-bodied persons. However, they can potentially recover their limb function because their nervous system circuitry is largely intact and is susceptible to reorganization through neurorehabilitation. FES and robot-based neurorehabilitation aim to induce reorganization through therapeutic exercises that are repeatable, flexible, and quantifiable. Because robotic devices are programmable, a variety of control strategies such as assist-as-needed control strategy and challenge-based training strategy (e.g., resistive training and error-augmentative control) are feasible with repetition [2]. Emphasis on a variety of control strategies is motivated from motor learning principles to improve the impact and outcome of robotic therapy [2].

However, ability of these control strategies to strongly induce neuroplasticity and motor learning is dependent on the measure of weakened voluntary effort. The measurement of true human voluntary effort evokes correct modulation of robotic or FES response as per the prescribed control strategy. Due to the limitations of the existing non-invasive sensing modalities, it is often difficult to reliably predict the weakened voluntary effort of persons with iSCI. Noninvasive electromyography (EMG) signal is commonly used as a prediction of the voluntary muscle force or corresponding joint torque [3]–[5]. However, it cannot reliably detect human intent due to its susceptibility to interference from signals of neighboring muscles and artifacts from FES. We propose that ultrasound (US) imaging can be used to predict the voluntary effort due to its primary advantage of providing direct visualization and measurement of muscles that govern gait function. The US-based sensing method can greatly overcome the drawbacks of using EMG method [5], but the information extraction from US imaging at a high sampling frequency is challenging. For example in [5], the video output of B-mode US scanner was digitized with a rate of 8 frames per second.

In this paper, we focus on designing a state observer to estimate volitional ankle joint movements. The EMG signal is assumed as the volitional signal from the central nervous system. A signal measured from US imaging is regarded as the level of muscle activation. Besides, an inertial measurement unit (IMU) is utilized to measure the angular velocity of the ankle joint. These signals are given as inputs to a nonlinear continuous time neuromuscular model that is used in the dynamics-based observer to predict ankle state. Since IMU signals can be sampled and processed at a higher sampling frequency than the US imaging-derived signals, it is harder to synchronize the two signals. The US-derived signals are sampled at a lower rate due to imaging processing and information extraction from the US raw signals. However, for each measurement, there is an allowable maximum value of sampling period (AMSP) and an allowable maximum value of output delay (AMOD).

Clearly, a state observer for the aforementioned volition

Qiang Zhang, Zhiyu Sheng, Kang Kim and Nitin Sharma are with the Department of Mechanical Engineering and Materials Science, University of Pittsburgh School of Engineering, Pittsburgh, PA, USA. (e-mail: qiz81@pitt.edu, zhs41@pitt.edu, kangkim@upmc.edu, and nis62@pitt.edu). Kang Kim and Nitin Sharma are also with the Department of Bioengineering, University of Pittsburgh School of Engineering, Pittsburgh, PA, USA. Kang Kim is also with the Center for Ultrasound Molecular Imaging and Therapeutics-Department of Medicine and Heart and Vascular Institute, University of Pittsburgh School of Medicine and University of Pittsburgh Medical Center, Pittsburgh, PA, USA. Kang Kim is also with the McGowan Institute for Regenerative Medicine, University of Pittsburgh and University of Pittsburgh Medical Center, Pittsburgh, PA, USA. This work was funded by NSF CAREER Award # 1750748.

prediction problem must process information from several sensors that work at different sampling rates. Moreover, synchronization among multi-sampling rates is hard to maintain due to possible delays in processing. These type of problems have led to the design of multi-rate observer designs, which has received great attention for linear systems. In [6], a controller synthesis technique for linear multi-rate sampled-data systems by pole placement was studied. A novel sufficient Krasovskii-based stability criteria for linear multi-rate sampled-data systems with uncertain sampling interval was proposed. The stability criteria were cast as linear matrix inequalities (LMI) [7]. In [8], the authors proposed a multi-rate estimator for linear systems, which is based on the continuous-time Luenberger observer method plus an inter-sample predictor for each sampled output measurement. Authors in [9] investigated a Kalman filter adaptation for a linear continuous-discrete system with multi-rate sampling time output. They considered the update step that occurred only when the sampled measurements were available. In [10], an estimator based on a multi-rate moving horizon estimation (MHE) strategy was proposed, and the missing sample of the slow measurement was compensated by a prediction value.

For a more complex situation, the observer design for nonlinear dynamic systems with multi-rate sampled output measurements cannot be solved by the aforementioned methods. Recently new contributions have been made in the area of multi-rate observers for nonlinear systems. In [11], for a class of triangular nonlinear systems, the authors used a Lyapunov approach to guarantee an exponential convergence of the observation error and improved the bounds of a maximum allowable transfer interval compared to the small gain approach. In [12], the authors designed a multi-rate observer that is based on a continuous-time design coupled with the inter-sample predictors for each sampled measurements. The error dynamics of the hybrid system was input-to-output stable by applying Krafyllis-Jiang vector small gain theorem. In [13], the authors built an observer for a multi input-multi output nonlinear system with multi-rate sampled and delayed measurements.

The main contributions of this work are summarized as follows. 1) Under several assumptions, a continuous time state observer is designed for a general nonlinear neuromuscular system with multi-rate sampled and uncertain delayed output measurements. The update law is designed to combine two sensory measurements instead of using only one sensor measurement. 2) Based on Lyapunov-Krasovskii function, the maximum allowable transfer interval is derived to guarantee exponential convergence of the observation error.

II. Modeling

The continuous-time dynamics of the ankle model, as shown in Fig. 1, can be expressed as

$$J\ddot{\varphi}(t) + mgLsin(\varphi(t)) + \tau_p(t) = \tau_{an}(t), \tag{1}$$

where $J \in \mathbb{R}$ and $m \in \mathbb{R}$ are the moment of inertia and the mass of human foot, respectively, $g \in \mathbb{R}$ is the gravitational acceleration, $L \in \mathbb{R}$ is the length from ankle to the center of the mass. $\varphi(t), \dot{\varphi}(t), \ddot{\varphi}(t) \in \mathbb{R}$ are the anatomical ankle angular position, velocity, and acceleration. $\tau_p(t) \in \mathbb{R}$ denotes the passive musculoskeletal torque of the ankle joint, and $\tau_{an}(t) \in \mathbb{R}$ denotes the torque generated by the voluntary contraction of the TA muscle.

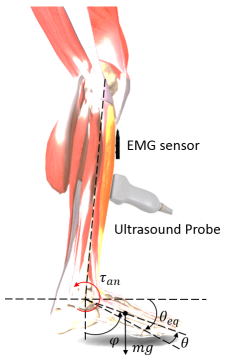

Figure 1. Ankle dynamic model for voluntary TA contraction

The passive and active TA muscle torques of the human ankle are modeled as [14]

$$\begin{aligned}\tau_p(t) &= d_1(\varphi(t) - \varphi_0(t)) + d_2\dot{\varphi}(t) \\ &\quad + d_3 e^{d_4\varphi(t)} - d_5 e^{d_6\varphi(t)},\end{aligned} \tag{2}$$

$$\tau_{an}(t) = (c_2\varphi^2(t) + c_1\varphi(t) + c_0)(1 + c_3\dot{\varphi}(t))a_{an}(t). \tag{3}$$

The coefficients $d_i \in \mathbb{R}$ $(i = 1, 2, ..., 6)$, $c_j \in \mathbb{R}$ $(j = 1, 2, 3)$, and $\varphi_0 \in \mathbb{R}$ are specific parameters for individual subject. $a_{an}(t) \in$[0,1] denotes the normalized TA muscle activation represented by the normalized parameter from US images. The normalized muscle activation dynamics are given as [15] [16]

$$\dot{a}_{an}(t) = \frac{u_{an}(t) - a_{an}(t)}{T_a}, \tag{4}$$

where $u_{an}(t) \in [0, 1]$ denotes the normalized excitation, and $T_a \in \mathbb{R}$ is the TA muscle contraction time constant. In (3), a_{an} and u_{an} are measured from the processed US images and processed EMG signal, respectively, and satisfy the following assumptions:

Assumption 1: The normalized excitation term is a linear function of the processed EMG signal, and the normalized muscle activation term is a linear function of the processed US images

$$u_{an}(t) = \frac{Q(t) - Q_{\min}}{Q_{\max} - Q_{\min}}, \; a_{an}(t) = \frac{\beta(t) - \beta_{\min}}{\beta_{\max} - \beta_{\min}}, \tag{5}$$

where $Q(t)$ is also called moving root mean square (MRMS) [17] and is given as

$$Q(t) = rms\{l(t)\} = \left(\frac{1}{T}\int_t^{t+T} l^2(t)dt\right)^{1/2}, \tag{6}$$

where $t \in \mathbb{R}$, $T \in \mathbb{R}$ and $l(t) \in \mathbb{R}$ represent the starting sampling time point, moving time window, and amplitude of EMG signal, respectively, $Q_{\min}$ and $Q_{\max}$ denote the minimum and maximum value of the MRMS, respectively.

$\beta(t) \in \mathbb{R}^+$ donates the information from US images. $\beta_{\min}$ and $\beta_{\max}$ denote the minimum and maximum value of $\beta(t)$, respectively.

By defining $x = [x_1, x_2, x_3]^{\mathrm{T}} = [\varphi, \dot{\varphi}, a_{an}]^{\mathrm{T}}$, the ankle joint nonlinear dynamic model in a state space form is

$$\dot{x}(t) = A(u_{an}(t), z(t))x(t) + Bu_{an}(t), \tag{7}$$

where

$$A(u_{an}(t), z(t))x(t) = \begin{bmatrix} x_2(t) \\ \frac{1}{J}(\tau_{an} - \tau_p - mgLsin(x_1(t))) \\ -\frac{x_3(t)}{T_a} \end{bmatrix},$$
$$B = \begin{bmatrix} 0 & 0 & \frac{1}{T_a} \end{bmatrix}^{\mathrm{T}},$$
$$\tau_{an}(t) = (c_2x_1^2(t) + c_1x_1(t) + c_0)(1 + c_3x_2(t))x_3(t),$$
$$\tau_p(t) = d_1(x_1(t) - \varphi_0) + d_2x_2(t) + d_3e^{d_4x_1(t)} - d_5e^{d_6x_1(t)}.$$

In continuous time, the measurements are angular velocity $x_2(t)$ and normalized muscle activation $x_3(t)$. The measurement model is

$$z(t) = Cx(t),\ y(t) = z(t-d) = Cx(t-d), \tag{8}$$

where $C = \begin{bmatrix} 0 & 1 & 0 \\ 0 & 0 & 1 \end{bmatrix}$ is a constant output matrix, $z(t) \in \mathbb{R}^2$ and $y(t) \in \mathbb{R}^2$ are the undelayed and delayed continuous time output measurements, respectively. $d \in \mathbb{R}^2$ is the output measurements delay for the sensor channels.

III. Observer design

The objective is to design an observer, $\hat{x}(t)$, for the nonlinear system with multi-rate sampled and unknown delayed measurements, such that the estimator error $e(t) = x(t) - \hat{x}(t)$ converges exponentially to the origin. We assume that the output measurements are sampled at time instants $t_k^i \in \mathbb{R}$, where $i = 1, 2$ represents there are 2 sensor channels, and $t_k^i < t_{k+1}^i (k = 0, 1, 2, ..., \infty)$ means that $\{t_k^i\}$ are monotonically increasing sequences and satisfy $\lim_{k\to\infty} t_k^i = \infty$. The ratio between sampling periods of the two channels is not necessarily an integer. In addition, due to the measurements delays, the sampled measurements are available at instants $t_k^i + \tau_k^i \in \mathbb{R}$, where $\tau_k^i \in \mathbb{R}^+$ denotes the unknown transmission delay on i^{th} sensor. It is noted that there is a upper bound $\bar{\tau}_i = \sup_{0\le k<\infty} (t_{k+1}^i - t_k^i)$ for all i and k. The sampled and delayed output measurements are given by

$$y_d(t_k^i) = z_d(t_k^i - \tau_k^i) = \begin{bmatrix} y_{d_1}(t_k^1) \\ y_{d_2}(t_k^2) \end{bmatrix} = \begin{bmatrix} \dot{\varphi}(t_k^1 - \tau_k^1) \\ a_{an}(t_k^2 - \tau_k^2) \end{bmatrix}. \tag{9}$$

The state space form in (7) can be considered as a more general lower triangular form

$$\begin{cases} \dot{x}_1(t) &= x_2(t) + f_1(x_1(t)) \\ \dot{x}_2(t) &= x_3(t) + f_2(x_1(t), x_2(t)) \\ \dot{x}_3(t) &= f_3(x_1(t), x_2(t), x_3(t)) + u(t) \\ z(t) &= \begin{bmatrix} x_2(t) & x_3(t) \end{bmatrix}^{\mathrm{T}} \\ & t \in \begin{bmatrix} t_k & t_{k+1} \end{bmatrix}, k \ge 0 \\ y_d(t_k^i) &= \begin{bmatrix} x_2(t_k^1 - \tau_k^1) & x_3(t_k^2 - \tau_k^2) \end{bmatrix}^{\mathrm{T}} \end{cases}, \tag{10}$$

where $u(t)$ is the input, $f_j(\cdot)(j = 1, 2, 3)$ is the remainder term after extraction of the corresponding state variable, and it satisfies the globally Lipschitz condition, which can be given as

$$\begin{aligned} &|f_j(x_1, \ldots, x_j) - f_j(\hat{x}_1, \ldots, \hat{x}_j)| \\ &\le r(|x_1 - \hat{x}_1| + \ldots + |x_j - \hat{x}_j|) \end{aligned}, \tag{11}$$

where r is a positive constant.

Lemma 1. *For any given positive definite matrix $M \in \mathbb{R}^{n\times n}$, a scalar $\alpha > 0$, and a vector function v, the following inequality is defined as [18]*

$$\left[\int_0^\alpha v(s)ds\right]^{\mathrm{T}} M \left[\int_0^\alpha v(s)ds\right] \le \alpha \left[\int_0^\alpha v(s)^{\mathrm{T}} M v(s)ds\right]. \tag{12}$$

For the system (10), the following observer is designed

$$\begin{cases} \dot{\hat{x}}_1(t) &= \hat{x}_2(t) + f_1(\hat{x}_1(t)) \\ & \quad +\gamma_1\left(e_2(t_k^1) + \frac{e_3(t_k^2)}{E}\right) \\ \dot{\hat{x}}_2(t) &= \hat{x}_3(t) + f_2(\hat{x}_1(t), \hat{x}_2(t)) \\ & \quad +\gamma_2\left(Ee_2(t_k^1) + e_3(t_k^2)\right) \\ \dot{\hat{x}}_3(t) &= f_3(\hat{x}_1(t), \hat{x}_2(t), \hat{x}_3(t)) \\ & \quad +\gamma_3\left(E^2e_2(t_k^1) + Ee_3(t_k^2)\right) + u(t) \\ \hat{x}_j(t_{k+1}^i + \tau_{k+1}^i) &= \lim_{t\to t_{k+1}^i+\tau_{k+1}^i{}^-} \hat{x}_j(t), \\ & \quad \forall i = 1, 2,\ \forall j = 1, 2, 3 \\ t &\in \left[t_k^i + \tau_k^i, t_{k+1}^i + \tau_{k+1}^i\right), k \ge 0 \end{cases}, \tag{13}$$

where $\hat{x}_j(t) = \hat{x}_{j_0}$ for $t \in \left[t_0, t_0 + \tau_0^i\right]$ $(t_0 = t_0^i)(i = 1, 2)$ $e_{i+1}(t_k^i) = y_{d_i}(t_k^i) - c_{i,i+1}\hat{x}_{i+1}(t_k^i)$ $(\forall i = 1, 2)$, $c_{i,i+1}$ is the i^{th} row and $(i+1)^{th}$ column element of C. $E \ge 1$ and $\gamma_j (j = 1, 2, 3)$ are positive constant values that are subsequently defined. The estimation errors of the state variables are defined as

$$e_j(t) = x_j(t) - \hat{x}_j(t),\ j = 1, 2, 3. \tag{14}$$

At the same time, the definition of global exponential convergence for the system (13) is equivalent to the exponential stability of estimation error dynamics, which is given as follows [13].

Definition 1. The observer (13) is said to be exponentially stable, if there exits a non-decreasing function S and a positive constant ξ such that $\|x(t) - \hat{x}(t)\| \le \exp(-\xi(t - t_0))S(\|x_0\|, \|\hat{x}_0\|)$ for any given $x_0 \in \mathbb{R}^n$ and $\hat{x}_0 \in \mathbb{R}^n$.

The outputs $y_d(t_k^i)$ can be measured by two sensor channels. Although the time delay τ_k^i for each channel is not known, the data from the sensors is sampled at instants t_k^i, and the evolution process $e_{i+1}(t_k^i) = y_{d_i}(t_k^i) - c_{i,i+1}\hat{x}_{i+1}(t_k^i)$ $(\forall i = 1, 2)$ is updated at instants $t_k^i + \tau_k^i$, which means $e_2(t_k^1)$ and $e_3(t_k^2)$ are updated automatically once the output $y_d(t_k^i)$ is available. Otherwise, during the time period $t \in \left[t_k^i + \tau_k^i, t_{k+1}^i + \tau_{k+1}^i\right)$, $e_2(t)$ and $e_3(t)$ will stay as two continuous functions.

Definition 2. Based on the above modeling, the estimation error dynamics is presented as follows

$$\begin{cases} \dot{e}_1(t) = e_2(t) - \gamma_1\left(e_2(t_k^1) + \frac{e_3(t_k^2)}{E}\right) + \tilde{f}_1 \\ \dot{e}_2(t) = e_3(t) - \gamma_2\left(Ee_2(t_k^1) + e_3(t_k^2)\right) + \tilde{f}_2 \\ \dot{e}_3(t) = -\gamma_3\left(E^2e_2(t_k^1) + Ee_3(t_k^2)\right) + \tilde{f}_3 \\ e_j(t_{k+1}^i + \tau_{k+1}^i) = \lim_{t\to t_{k+1}^i+\tau_{k+1}^i{}^-} \hat{e}_j(t),\ i = 1, 2 \\ j = 1, 2, 3,\ t \in \left[t_k^i + \tau_k^i, t_{k+1}^i + \tau_{k+1}^i\right), k \ge 0 \end{cases}, \tag{15}$$

where $\tilde{f}_j = f_j(x_1(t),\ldots,x_j(t)) - f_j(\hat{x}_1(t),\ldots,\hat{x}_j(t))$ $(\forall j = 1,2,3)$ are the corresponding errors of nonlinear terms. $\gamma_j (j = 1,2,3)$ are the parameters that satisfy the following inequality

$$\Gamma^{\mathrm{T}} P + P\Gamma \leq -I, \tag{16}$$

where $\Gamma = \begin{bmatrix} -\gamma_1 & 1 & 0 \\ -\gamma_2 & 0 & 1 \\ -\gamma_3 & 0 & 0 \end{bmatrix}$, and $P = P^T \in \mathbb{R}^{3\times 3}$ is positive definite matrix.

IV. Convergence and Simulation Results

A. Convergence Analysis

To find the sufficient conditions for the observer (13) to converge exponentially, several assumptions are given [19]:

Assumption 2: All system signals (x, y, z, u_{an}) are bounded and there is a known upper bound y_M for the output amplitude $\|y(t)\|$.

Assumption 3: The pair $(A(u_{an}(t), z(t)), C)$ is uniformly observable.

Assumption 4: The output delay value AMOD should be less than the sampling time AMSP, which means that the measurements sampled at instants t_k^i can be used for the current observer design before the next measurements come at instants t_{k+1}^i.

Define a varying delay variable $\delta_i(t) = t - t_k^i, t \in \left[t_k^i + \tau_k^i, t_{k+1}^i + \tau_{k+1}^i\right)$. Then, the term t_k^i can be expressed as $t_k^i = t - \delta_i(t)$. It is obvious that $0 < \delta_i(t) = t - t_k^i < t_{k+1}^i + \tau_{k+1}^i - t_k^i < \epsilon$, where $\epsilon > 0$. The goal of the proof is to find the upper bounds of ϵ such that the error dynamics system (15) is globally exponentially stable. In addition, the following coordinates $\begin{cases} \varepsilon_1(t) = \frac{e_1(t)}{E} \\ \varepsilon_2(t) = \frac{e_2(t)}{E^2} \\ \varepsilon_3(t) = \frac{e_3(t)}{E^3} \end{cases}$ are used for substitution in error dynamics (15) , which turns out to be

$$\begin{cases} \dot{\varepsilon}_1(t) &= E\gamma_1\left(\int_{t-\delta_1(t)}^{t} \dot{\varepsilon}_2(s)ds + \int_{t-\delta_2(t)}^{t} \dot{\varepsilon}_3(s)ds\right) \\ & +E\varepsilon_2(t)\ -E\gamma_1\left(\varepsilon_2(t) + \varepsilon_3(t)\right) + \frac{\tilde{f}_1}{E} \\ \dot{\varepsilon}_2(t) &= E\gamma_2\left(\int_{t-\delta_1(t)}^{t} \dot{\varepsilon}_2(s)ds + \int_{t-\delta_2(t)}^{t} \dot{\varepsilon}_3(s)ds\right) \\ & +E\varepsilon_3(t)\ -E\gamma_2\left(\varepsilon_2(t) + \varepsilon_3(t)\right) + \frac{\tilde{f}_2}{E^2} \\ \dot{\varepsilon}_3(t) &= E\gamma_3\left(\int_{t-\delta_1(t)}^{t} \dot{\varepsilon}_2(s)ds + \int_{t-\delta_2(t)}^{t} \dot{\varepsilon}_3(s)ds\right) \\ & -E\gamma_3\left(\varepsilon_2(t) + \varepsilon_3(t)\right) + \frac{\tilde{f}_3}{E^3} \end{cases}. \tag{17}$$

Theorem 1. *In the system (10) with the globally Lipschitz condition in (11), based on the inequality (16), $\gamma_j > 0 (j = 1,2,3)$, if E and ϵ satisfy the following conditions*

$$E > \max\left\{1, r, 64r\bar{p}\right\}, \tag{18}$$

$$\epsilon < \min\left\{\frac{1}{36E\left(1+\bar{\gamma}^2\right)}, \frac{-\bar{\lambda}^2 + \sqrt{\bar{\lambda}^4 + 3}}{6E\bar{\gamma}}\right\}, \tag{19}$$

then, the system (13) is said to be a globally exponentially stable observer for the system (10), where $\bar{p} = \max\left\{|P_{mn}|\right\}(m,n = 1,2,3)$, P_{mn} is the m^{th} row and n^{th} column element of matrix P. $\bar{\lambda} = \lambda_{\max}(P)$ and $\bar{\gamma} = \max\left\{\gamma_j\right\}(j = 1,2,3)$.

Proof: Consider a positive definite function as follows

$$V_1(t) = \varepsilon(t)^{\mathrm{T}} P \varepsilon(t), \tag{20}$$

where $\varepsilon(t) = [\varepsilon_1(t), \varepsilon_2(t), \varepsilon_3(t)]^{\mathrm{T}}$, and the time interval is set as $t \in \left[t_k^i + \tau_k^i, t_{k+1}^i + \tau_{k+1}^i\right)$. According to [13], the derivative of $V_1(t)$ along the system (17) is presented as

$$\begin{aligned} \frac{dV_1(t)}{dt} &= \dot{\varepsilon}(t)^{\mathrm{T}} P\varepsilon(t) + \varepsilon(t)^{\mathrm{T}} P\dot{\varepsilon}(t) \\ &\leq -E\varepsilon(t)^{\mathrm{T}}\varepsilon(t) \\ &\quad +2r\sum_{m=1}^{3}\sum_{n=1}^{3}\left|\varepsilon_m(t)P_{mn}\right|\left(\left|\varepsilon_1(t)\right| \right. \\ &\quad \left. +\ldots+\left|\varepsilon_n(t)\right|\right)+ \\ &\quad 2\left(\sum_{m=1}^{3}\sum_{n=1}^{3} E\varepsilon_m(t)\left(P_{mn}\gamma_n\right)\left(\int_{t-\delta_1(t)}^{t}\dot{\varepsilon}_2(s)ds \right.\right. \\ &\quad \left.\left. +\int_{t-\delta_2(t)}^{t}\dot{\varepsilon}_3(s)ds\right)\right) \\ &\leq -E\varepsilon(t)^{\mathrm{T}}\varepsilon(t) + \frac{1}{4}E\varepsilon(t)^{\mathrm{T}}\varepsilon(t) \\ &\quad +2r\bar{p}8\varepsilon(t)^{\mathrm{T}}\varepsilon(t) + 4E\left(\bar{\lambda}\right)^2\bar{\gamma}\left(\left(\int_{t-\delta_1(t)}^{t}\dot{\varepsilon}_2(s)ds\right)^2\right. \\ &\quad \left. +\left(\int_{t-\delta_2(t)}^{t}\dot{\varepsilon}_3(s)ds\right)^2\right) \\ &\leq -\frac{3}{4}E\varepsilon(t)^{\mathrm{T}}\varepsilon(t) + 16r\bar{p}\varepsilon(t)^{\mathrm{T}}\varepsilon(t) + \\ &\quad 4E\left(\bar{\lambda}\right)^2\bar{\gamma}\left(\left(\int_{t-\delta_1(t)}^{t}\dot{\varepsilon}_2(s)ds\right)^2\right. \\ &\quad \left. +\left(\int_{t-\delta_2(t)}^{t}\dot{\varepsilon}_3(s)ds\right)^2\right). \end{aligned} \tag{21}$$

From (18), the above equation can be expressed as

$$\begin{aligned} \frac{dV_1(t)}{dt} &\leq -\frac{1}{2}E\varepsilon(t)^{\mathrm{T}}\varepsilon(t) + \\ &\quad 4E\left(\bar{\lambda}\right)^2\bar{\gamma}\left(\left(\int_{t-\delta_1(t)}^{t}\dot{\varepsilon}_2(s)ds\right)^2\right. \\ &\quad \left. +\left(\int_{t-\delta_2(t)}^{t}\dot{\varepsilon}_3(s)ds\right)^2\right). \end{aligned} \tag{22}$$

As mentioned in Lemma 1, let $\delta(t) = \max\{\delta_1(t), \delta_2(t)\}$, the inequality (22) can be given as

$$\begin{aligned} \frac{dV_1(t)}{dt} &\leq -\frac{1}{2}E\varepsilon(t)^{\mathrm{T}}\varepsilon(t) \\ &\quad +4\delta(t)E\left(\bar{\lambda}\right)^2\bar{\gamma}\left(\int_{t-\delta_1(t)}^{t}\left(\dot{\varepsilon}_2(s)\right)^2 ds\right. \\ &\quad \left. +\int_{t-\delta_2(t)}^{t}\left(\dot{\varepsilon}_3(s)\right)^2 ds\right) \\ &\leq -\frac{1}{2}E\varepsilon(t)^{\mathrm{T}}\varepsilon(t) \\ &\quad +4\epsilon E\left(\bar{\lambda}\right)^2\bar{\gamma}\left(\int_{t-\epsilon}^{t}\left(\left(\dot{\varepsilon}_2(s)\right)^2\right.\right. \\ &\quad \left.\left. +\left(\dot{\varepsilon}_3(s)\right)^2\right)ds\right). \end{aligned} \tag{23}$$

Here, another positive definite function called auxiliary integral function is constructed as follows

$$V_2(t) = \int_{t-\epsilon}^{t}\int_{\varrho}^{t} \left((\dot{\varepsilon}_2(s))^2 + (\dot{\varepsilon}_3(s))^2\right) ds d\varrho, t \geq t_0 + \epsilon. \quad (24)$$

Based on Lemma 1, it is clear that $V_2(t) \leq \epsilon \int_{t-\epsilon}^{t} \left((\dot{\varepsilon}_2(s))^2 + (\dot{\varepsilon}_3(s))^2\right) ds$. Then based on Leibniz integral rule, take the derivative of $V_2(t)$ we can get

$$\frac{dV_2(t)}{dt} = \epsilon \left((\dot{\varepsilon}_2(t))^2 + (\dot{\varepsilon}_3(t))^2\right) - \int_{t-\epsilon}^{t} \left((\dot{\varepsilon}_2(s))^2 + (\dot{\varepsilon}_3(s))^2\right) ds. \quad (25)$$

From (19), we can get

$$\begin{aligned}
\frac{dV_2(t)}{dt} &\leq \epsilon \sum_{j=1}^{3} (\dot{\varepsilon}_j(t))^2 + \int_{t-\epsilon}^{t} \left((\dot{\varepsilon}_2(s))^2 + (\dot{\varepsilon}_3(s))^2\right) ds \\
&= \epsilon \Bigg(E\varepsilon_2(t) + E\gamma_1 \Big(\int_{t-\delta_1(t)}^{t} \dot{\varepsilon}_2(s) ds \\
&\quad + \int_{t-\delta_2(t)}^{t} \dot{\varepsilon}_3(s) ds \Big) - E\gamma_1 \left(\varepsilon_2(t) + \varepsilon_3(t)\right) + \frac{\tilde{f}_1}{E} \Bigg)^2 \\
&\quad + \epsilon \Bigg(E\varepsilon_3(t) + E\gamma_2 \Big(\int_{t-\delta_1(t)}^{t} \dot{\varepsilon}_2(s) ds \\
&\quad + \int_{t-\delta_2(t)}^{t} \dot{\varepsilon}_3(s) ds \Big) - E\gamma_2 \left(\varepsilon_2(t) + \varepsilon_3(t)\right) + \frac{\tilde{f}_2}{E^2} \Bigg)^2 \\
&\quad + \epsilon \Bigg(E\gamma_3 \Big(\int_{t-\delta_1(t)}^{t} \dot{\varepsilon}_2(s) ds + \int_{t-\delta_2(t)}^{t} \dot{\varepsilon}_3(s) ds \Big) \\
&\quad - E\gamma_3 \left(\varepsilon_2(t) + \varepsilon_3(t)\right) + \frac{\tilde{f}_3}{E^3} \Bigg)^2 \\
&\quad - \int_{t-\epsilon}^{t} \left((\dot{\varepsilon}_2(s))^2 + (\dot{\varepsilon}_3(s))^2\right) ds \\
&\leq 3\epsilon E^2 \Big(|\varepsilon_1(t)| + |\varepsilon_2(t)| + |\varepsilon_3(t)| + \bar{\gamma} |\varepsilon_1(t)| \\
&\quad + \bar{\gamma} |\varepsilon_2(t)| + \bar{\gamma} |\varepsilon_3(t)| + \bar{\gamma} \int_{t-\epsilon}^{t} \Big| \dot{\varepsilon}_2(s) \Big| ds \\
&\quad + \bar{\gamma} \int_{t-\epsilon}^{t} \Big| \dot{\varepsilon}_3(s) \Big| ds \Big)^2 \\
&\quad - \int_{t-\epsilon}^{t} \left((\dot{\varepsilon}_2(s))^2 + (\dot{\varepsilon}_3(s))^2\right) ds \\
&\leq \left(12\epsilon^2 E^2 (\bar{\gamma})^2 - 1\right) \int_{t-\epsilon}^{t} \left((\dot{\varepsilon}_2(s))^2 + (\dot{\varepsilon}_3(s))^2\right) ds \\
&\quad + 18\epsilon E^2 (1+\bar{\gamma})^2 \varepsilon(t)^{\mathrm{T}} \varepsilon(t). \quad (26)
\end{aligned}$$

Given the above analysis, now we can construct the Lyapunov-Krasovskii candidate

$$V(t) = V_1(t) + V_2(t), t \geq t_0 + \bar{\epsilon}. \quad (27)$$

Then, from inequalities (23) and (25), it can be obtained

$$\begin{aligned}
\frac{dV(t)}{dt} &\leq \left(-\frac{1}{2}E + 18\epsilon E^2 (1+\bar{\gamma})^2\right) \varepsilon(t)^{\mathrm{T}} \varepsilon(t) \\
&\quad + \left(4\epsilon E \bar{\lambda}^2 \bar{\gamma} + 12\epsilon^2 E^2 \bar{\gamma}^2 - 1\right) \\
&\quad \left(\int_{t-\epsilon_i}^{t} \left(\dot{\varepsilon}_{i+1}^{i}(s) \right)^2 ds \right). \quad (28)
\end{aligned}$$

Substitute the sufficient conditions in Theorem 1 and the above inequality will turn out to $\frac{dV(t)}{dt} < 0$. Furthermore, the form in (28) can also be expressed as

$$\frac{dV(t)}{dt} \leq \varsigma_1 V_1(t) + \varsigma_2 V_2(t) \quad (29)$$

where $\varsigma_1 = -\frac{1}{2}E + 18\epsilon E^2 (1+\bar{\gamma})^2 < 0$, and $\varsigma_2 = 4\epsilon E \bar{\lambda}^2 \bar{\gamma} + 12\epsilon^2 E^2 \bar{\gamma}^2 - 1 < 0$. Assume $\varsigma = \max\{\varsigma_1, \varsigma_2\} < 0$, then we can get

$$\frac{dV(t)}{dt} \leq \varsigma \left(V_1(t) + V_2(t)\right) \leq \varsigma V(t), t \geq t_0 + \epsilon. \quad (30)$$

Thereafter, $V(t) \leq \exp\left(\varsigma(t - t_0 - \epsilon)\right) V(t_0 + \epsilon)$. Up to now, the nonlinear neuromuscular system (10) and its observer (13) both have the global Lipschitz features, and then the sufficient conditions are built to guarantee the observer error exponentially stable, which means that there exits a non-decreasing function S and a positive constant ξ such that $\|x(t) - \hat{x}(t)\| \leq \exp(-\xi(t - t_0)) S(\|x_0\|, \|\hat{x}_0\|)$ for any given $x_0 \in \mathbb{R}^n$ and $\hat{x}_0 \in \mathbb{R}^n$. Therefore, the designed observer based on multi-rate sampled and delayed measurements is an exponentially stable observation method. ■

B. Simulation Results

The simulation for the nonlinear neuromuscular system (7) and (10) was performed in Matlab (R2017a, MathWorks). The parameters of the ankle dorsiflexion musculoskeletal model in the simulation are given in Table 1, and the parameters of the proposed observer are listed in Table 2.

As mentioned in section III, the sampling interval for each channel is not necessarily uniform, so let $t_k^1 = kT_1 - (0.2rand)T_1$ ($rand$ denotes random function in Matlab) and $t_k^2 = kT_2 - (0.3rand)T_2$ are the sampling sequences of two different channels, where T_1 and T_2 are positive constants as shown in Table 2. Also, the transmission delays of the two channels τ_k^1 and τ_k^2 are given by random numbers between interval (0, $0.5T_1$] and (0, $0.7T_2$]. Known all the parameters and by simple calculation, we can get $P = \begin{bmatrix} 3.526 & -0.5 & -2.654 \\ -0.5 & 2.654 & -0.5 \\ -2.654 & -0.5 & 3.208 \end{bmatrix}$, which is positive definite. Then, $\bar{\gamma} = 1.8$, $\bar{p} = 3.526$, and $\bar{\lambda} = 6.026$. Based on these parameters and Theorem 1, the other parameters can be derived $E = 2.26$, $\epsilon = 1.6 \times 10^{-3}$s. Fig.2 and Fig.3 show the simulation results of the estimation error convergence by the above set of parameters with the initial condition $x(0) = [-0.2rad, 0, 0]^{\mathrm{T}}$ and $\hat{x}(0) = [0, 0, 0]^{\mathrm{T}}$. Obviously, the state x_2 has the fastest convergence speed while state x_1 has the slowest one.

Table I
PARAMETERS OF THE ANKLE DORSIFLEXION MUSCULOSKELETAL MODEL

Parameter	m	g	L	φ_0	φ_{eq}
Value	0.96	9.81	0.1	0.18	1.22
Parameter	c_0	c_1	c_2	c_3	d_1
Value	56.85	39.83	-28.88	1.20	8.28
Parameter	d_2	d_3	d_4	d_5	d_6
Value	2.46	1.37×10^{-13}	18.07	10.56	-15.37
Parameter	T_a	J			
Value	0.14	0.0128			

Table II
PARAMETERS OF THE DESIGNED OBSERVER

Parameters	r	γ_1	γ_2	γ_3	T_1	T_2
Value	0.01	1.3	1.8	1.2	1×10^{-4}s	7×10^{-4}s

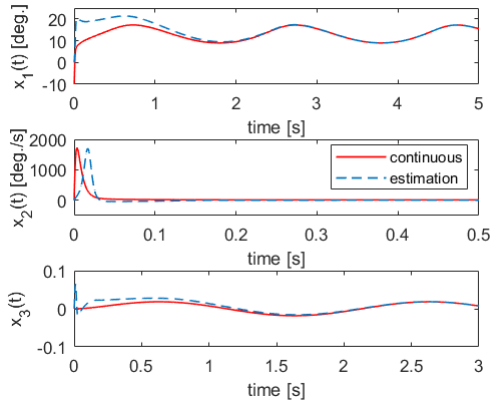

Figure 2. Ankle trajectories of the estimated states and continuous states

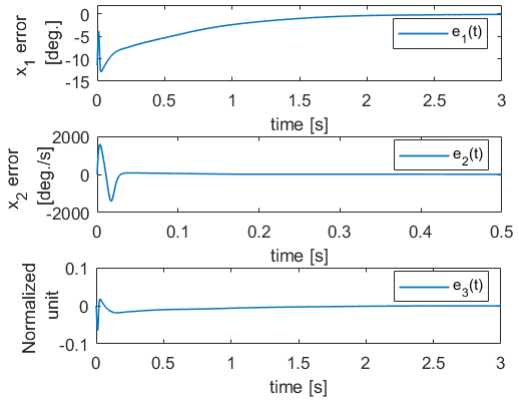

Figure 3. Ankle trajectories of estimated states error

V. CONCLUSION

In this paper, a continuous time observer was proposed for a nonlinear neuromuscular system with multi-rate sampled and non-uniform delayed measurements. The output measurements from an IMU sensor and processed ultrasound images have asynchronous sampling frequencies and uncertain delays. Under the assumptions that the both sampling intervals and delays have their respective allowable maximum values, sufficient conditions were derived based on a Lyapunov-Krasovskii function that can guarantee the exponential convergence of the observation error. Through simulations, the effectiveness of the proposed observer was verified. The proposed observer can help detect muscle activity, which can be used as the voluntary muscle effort prediction of people with iSCI. In the future work, experiments will be performed to verify the effectiveness of the proposed observer. Also, the proposed observer will be optimized to deal with a more general and complex situations, such as multi-rate sampled and delayed measurements with noise.

REFERENCES

[1] The National SCI Statistical Center, "Spinal cord injury (SCI) facts and figures at a glance," 2017.

[2] L. Marchal-Crespo and D. J. Reinkensmeyer, "Review of control strategies for robotic movement training after neurologic injury," *J Neuroeng Rehabil*, vol. 6, no. 1, p. 20, 2009.

[3] E. Wentink, S. Beijen, H. Hermens, J. Rietman, and P. Veltink, "Intention detection of gait initiation using EMG and kinematic data," *Gait & Posture*, vol. 37, no. 2, pp. 223–228, 2013.

[4] K. Nurhanim, I. Elamvazuthi, P. Vasant, T. Ganesan, S. Parasuraman, and M. K. Ahamed Khan, "Joint torque estimation model of surface electromyography(sEMG) based on swarm intelligence algorithm for robotic assistive device," in *Procedia Comput Sci*, vol. 42. Elsevier, 2014, pp. 175–182.

[5] J. Shi, Y. P. Zheng, Q. H. Huang, and X. Chen, "Continuous monitoring of sonomyography, electromyography and torque generated by normal upper arm muscles during isometric contraction: Sonomyography assessment for arm muscles," *IEEE Trans Biomed Eng*, vol. 55, no. 3, pp. 1191–1198, 2008.

[6] P. Colaneri, R. Scattolini, and N. Schiavoni, "Stabilization of multirate sampled-data linear systems," *Automatica*, vol. 26, no. 2, pp. 377–380, 1990.

[7] L. Rodrigues and M. Moarref, "Exponential stability and stabilization of linear multi-rate sampled-data systems Flight Management Systems View project Inverse Optimal Control View project Exponential Stability and Stabilization of Linear Multi-rate Sampled-data Systems," in *Proc ACC*. IEEE, 2013, pp. 158–163.

[8] C. Ling and C. Kravaris, "Multi-rate observer design for process monitoring using asynchronous inter-sample output predictions," *AIChE J*, vol. 63, no. 8, pp. 3384–3394, 2017.

[9] A. Feddaoui, N. Boizot, E. Busvelle, and V. Hugel, "A Kalman filter for linear continuous-discrete systems with asynchronous measurements," in *Proc IEEE CDC*. IEEE, 2017, pp. 2813–2818.

[10] A. Liu, W.-a. Zhang, L. Yu, and J. Chen, "Moving horizon estimation for multi-rate systems," in *Proc IEEE CDC*. IEEE, 2015, pp. 6850–6855.

[11] T. Ahmed-Ali, E. Cherrier, and F. Lamnabhi-Lagarrigue, "Cascade High Gain Predictors for a Class of Nonlinear Systems," *IEEE Trans Automat Contr*, vol. 57, no. 1, pp. 221–226, 2012.

[12] C. Ling and C. Kravaris, "Multi-rate sampled-data observers based on a continuous-time design," in *Proc. IEEE CDC*. IEEE, 2017, pp. 3664–3669.

[13] Y. Shen, D. Zhang, and X. Xia, "Continuous observer design for a class of multi-output nonlinear systems with multi-rate sampled and delayed output measurements," *Automatica*, vol. 75, pp. 127–132, 2017.

[14] D. Popović, R. Stein, M. Oğuztöreli, M. Lebiedowska, and S. Jonić, "Optimal control of walking with functional electrical stimulation: a computer simulation study," *IEEE Trans. Rehabil. Eng.*, vol. 7, no. 1, pp. 69–79, 1999.

[15] P. Veltink, H. Chizeck, P. Crago, and A. El-Bialy, "Nonlinear joint angle control for artificially stimulated muscle." *IEEE Trans. Biomed. Eng.*, vol. 39, no. 4, pp. 368–80, 1992.

[16] D. G. Thelen, "Adjustment of Muscle Mechanics Model Parameters to Simulate Dynamic Contractions in Older Adults," *J Biomech Eng*, vol. 125, no. 1, pp. 70–77, 2003.

[17] K. Watanabe and H. Akima, "Normalized EMG to normalized torque relationship of vastus intermedius muscle during isometric knee extension," *Eur. J. Appl. Physiol.*, vol. 106, no. 5, pp. 665–673, 2009.

[18] Y. Liu, Z. Wang, and X. Liu, "On global exponential stability of generalized stochastic neural networks with mixed time-delays," *Neurocomputing*, vol. 70, no. 1-3, pp. 314–326, 2006.

[19] M. Kahelras, T. Ahmed-Ali, T. Folin, F. Giri, and F. Lamnabhi-Lagarrigue, "Observer design for triangular nonlinear systems using delayed sampled-output measurements," in *Proc IEEE CDC*. IEEE, 2016, pp. 1447–1451.